SLAC-PUB-11242
May 2005

Weak FEL Gain Detection with a Modulated Laser-Based Beam Heater

P. Emma, Z. Huang, J. Wu
SLAC, Stanford, CA 94309, USA

Abstract

For an x-ray free-electron laser (FEL) such as the LCLS, the FEL gain signal is accompanied by spontaneous radiation with a significant power level. Detecting the weak FEL gain among the large spontaneous background in the early stage of the exponential growth or for a low quality electron beam is important in commissioning the FEL. In this paper, we describe a simple "lock-in" method of weak FEL gain detection, suggested by K. Robinson, accomplished by slowly modulating the laser power of a designated beam heater that controls the local energy spread of the electron beam. We present numerical modelling that shows the effectiveness of this method and discuss its implementation in the LCLS.

INTRODUCTION

The Linac Coherent Light Source (LCLS) [1] will be the world's first x-ray free electron laser (FEL) when it becomes operational in 2009. The high energy electrons used to drive the FEL interaction are also capable of generating intense incoherent undulator radiation over a wide spectral range. Detecting the FEL signal among the large spontaneous background can be a challenging issue, especially when the FEL gain is not very high if the electron beam qualities (such as the emittance) are worse than the design values and/or if the machine is not properly tuned. Thus, it is very important to develop techniques for weak FEL signal detection in order to fully characterize the electron beam and to optimize the machine.

In order to suppress the microbunching instability driven by longitudinal space charge and coherent synchrotron radiation effects in the accelerator system, the LCLS plans to use a designated laser heater that increases the incoherent energy spread of the beam generated by the photocathode rf gun [2]. The designed increase in the local energy spread by the laser heater is expected to damp the microbunching instability to a tolerable level while having a negligible impact on FEL performance. Increasing the local energy spread beyond the designated level starts to affect the FEL gain significantly. Since the local energy spread is easily controlled by the laser power level, it was suggested recently [3] that a modulated laser power will modulate the FEL power within the static spontaneous background and facilitate the FEL signal detection. In this paper, we study this signal "lock-in" method with numerical examples and discuss its implementation to the LCLS.

METHOD

We illustrate this "lock-in" method of signal detection with a hypothetical case when the FEL power is much lower than the background spontaneous radiation. We take the nominal LCLS parameters as shown in Table 1, except that we assume a much larger normalized transverse emittance $\gamma\varepsilon_x = \gamma\varepsilon_y = 3.6$ μm (instead of the desired 1.2-μm value). The power gain length, in this case, calculated by Xie's fitting formula [5] is about $L_G \approx 16$ m. The FEL power at the end of the undulator tunnel (with an active undulator distance $L_u = 112$ m) before saturation can be estimated by

$$P_{\rm FEL} \approx \frac{1}{9} P_n \exp\left(\frac{L_u}{L_G}\right), \qquad (1)$$

where

$$P_n \approx \sqrt{2\pi}\frac{\rho^2 \gamma mc^3}{\lambda_r} \qquad (2)$$

is the approximate start-up noise power in the one-dimensional FEL theory [6]. Equations (1) and (2) predict a mere 120-kW FEL power instead of the 10-GW saturation power expected from a beam with 1.2-μm normalized emittance. Assuming a radiation detector that has a 1% bandwidth around the fundamental wavelength λ_r, the spontaneous undulator radiation within this bandwidth is about 10 MW at the undulator end, completely dominating the FEL signal.

Nevertheless, the FEL signal is very sensitive to the local energy spread of the beam. The nominal rms energy spread of 1×10^{-4} at 13.6 GeV is obtained by the laser heater that induces about 40-keV rms energy spread at the injector end (135 MeV) prior to any bunch compression. For a laser spot size matching the electron transverse size, the required laser power is about $P_L \approx 1.2$ MW [2], a very small fraction of the unconverted infrared laser power of the photocathode drive laser. Since the laser-heated energy spread is proportional to $\sqrt{P_L}$, we can modulate the laser power in the laser heater between 1.2 MW and 19 MW at, for example, an unique 7-Hz rate. The laser heated rms energy spread is then modulated between 40 keV and 160 keV, before bunch compression, as shown in Fig. 1. Thus, the FEL power will modulate accordingly between 3 kW to 120 kW as also shown in Fig. 1, which can be distinguished from the unmodulated spontaneous power via Fast Fourier Transform (FFT). A square wave, rather than sinusoidal, modulation is used to improve the lock-in efficiency [4].

Contributed to Particle Accelerator Conference (PAC05), Knoxville, TN, May 16-20, 2005
Work supported by Department of Energy contract DE-AC02-76SF00515

Table 1: The LCLS parameters with a hypothetically large transverse emittance.

Parameter	Symbol	Value
electron energy	γmc^2	13.6 GeV
bunch charge	Q	1 nC
bunch current	I_{pk}	3.4 kA
flattop bunch duration	τ	290 fs
rms energy spread at 135 MeV	σ_E	40 keV
heater laser peak power	P_L	1.2 MW
machine repetition rate	f_0	120 Hz
rms energy spread at undulator	σ_E/E	1×10^{-4}
transverse norm. emittance	$\gamma\varepsilon_{x,y}$	3.6 μm
undulator mean beta function	$\beta_{x,y}$	30 m
undulator period	λ_u	0.03 m
undulator field	B	1.3 T
undulator parameter	K	3.5
active undulator length	L_u	112 m
FEL wavelength	λ_r	1.5 Å
FEL parameter	ρ	2.9×10^{-4}

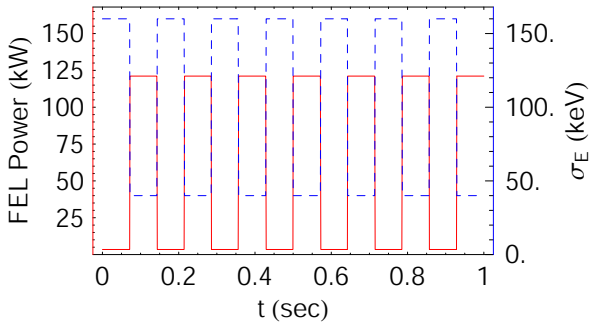

Figure 1: 7-Hz modulated laser-heated rms energy spread before bunch compression (dashed blue line) and FEL power signal (solid red line).

LCLS SIMULATIONS

In order to determine the worst case beam quality where lock-in detection is still possible, we model the LCLS conditions with parameters listed in Table 1. Furthermore, to include expected pulse-to-pulse variations in beam quality, we add random Gaussian variations of several key parameters such as bunch charge, RF phases, RF amplitudes, gun-timing, emittance, and noise on the radiation energy detector. These rms variations are listed in Table 2.

The LCLS accelerator is modelled using a fast, semi-analytical longitudinal phase space code which includes bunch compression to 2nd order, longitudinal wakefields, and beam/accelerator errors. The final parameters are plotted versus time in Fig. 2 over 10 seconds of machine operation at a 120-Hz pulse repetition rate. The figure shows the estimated FEL 3D gain length (using Xie's fitting formula [5]), the local energy spread at 13.6 GeV, the peak current in the undulator, and the normalized emittance. The

Table 2: RMS Gaussian random jitter errors applied to various parameters.

Parameter	Symbol	Value
relative bunch charge	$\Delta Q/Q$	2 %
electron gun-laser timing	Δt	0.5 ps
RF phase per linac	$\Delta\phi$	0.1 deg
RF amplitude per linac	$\Delta V/V_0$	0.1 %
transverse emittance (x and y)	$\Delta\varepsilon/\varepsilon$	4 %
radiation energy detector noise	$\Delta W/W$	1 %

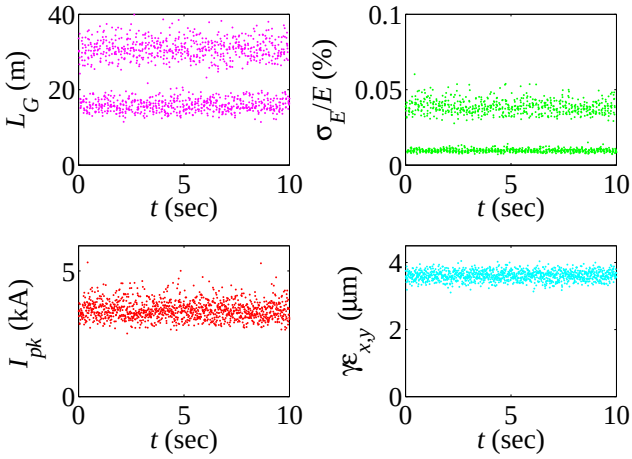

Figure 2: Gain length, local energy spread, peak current, and emittance over 10 seconds at 120-Hz, including square-wave heater modulation and beam jitter of Table 2.

effects of the laser-heater square-wave modulation can be seen in the gain length and local energy spread, which show two bands of values.

From this varying beam quality, the FEL and spontaneous power are simulated for each beam pulse. The total (FEL + spontaneous) 'measured' radiation energy per pulse (red) is plotted over 10 seconds in Fig. 3, including a 1% random detector noise. Also plotted is the weak FEL signal (blue) and the spontaneous radiation without detector noise (black). The only true observable quantity here is the total energy per pulse (red), which shows no clear 7-Hz modulation in this time-domain plot.

The weak FEL signal is easily detected in this large spontaneous background by applying an FFT to the total 'measured' radiation energy per pulse. The FFT is shown in Fig. 4, where a clear 7-Hz modulation is evident, providing an FEL signal, even with these very poor beam quality conditions, that might be used to begin tuning the machine.

The FEL gain can be estimated by using the amplitude of the FFT peak (in this case $W_0^2 \approx 400\ \mu\text{J}^2$), where an independent measurement of the full-width electron pulse duration, τ (for example using a transverse RF deflecting cavity [7]), is used to estimate the peak FEL power.

$$P_{pk} \approx \frac{\pi W_0}{2\Delta T f_0 \tau} \tag{3}$$

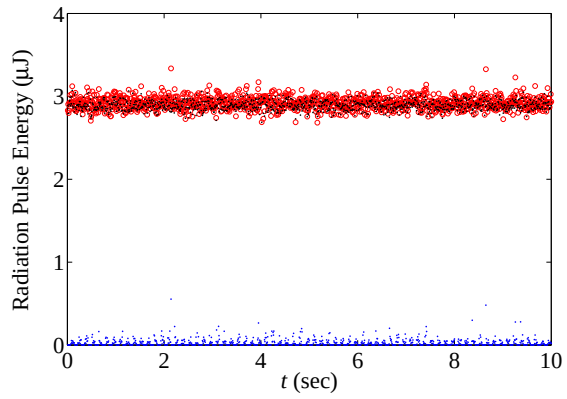

Figure 3: Total 'measured' radiation energy per pulse (red), weak FEL signal (blue), and spontaneous radiation (black), over 10 seconds of machine operation.

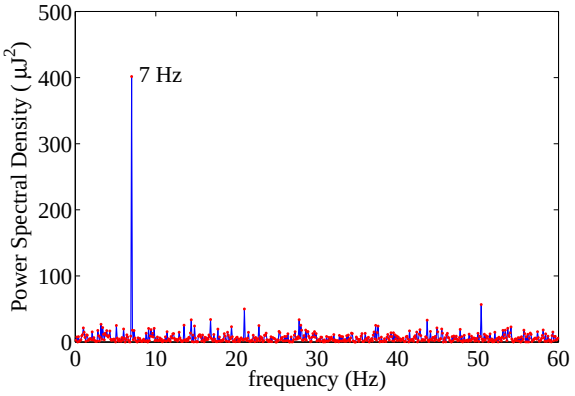

Figure 4: FFT of total 'measured' radiation energy from Fig. 3. The 7-Hz peak represents an FEL signal available for initial machine tuning.

Here ΔT is the data sample interval (10 seconds), f_0 is the machine repetition rate (120 Hz), and the factor $\pi/2$ derives from the square-wave modulation shown in Fig. 1. Equation (3) yields $P_{pk} \approx 180$ kW if the full-width electron pulse duration is $\tau \approx 290$ fs. This power level is somewhat larger than the theoretical expectation of 120 kW since fluctuations in electron beam quality bias toward a stronger mean FEL signal due to the exponential dependence.

The input seed power is estimated from Eq. (2), and the FEL gain is $G \approx P_{pk}/P_n$, or about 200 in this case.

DISCUSSIONS

With a smaller emittance, the FEL gain length, L_G, can also be estimated at an early stage along the undulator where the gain is still very small. The FEL gain can be suppressed after any particular point along the undulator by transversely kicking the electron beam at sequential quadrupole locations (every 4 meters) and recording the FFT peak amplitude at the lock-in frequency for each kick location. The FFT can be repeated a number of times for each kick location. The gain length can then be calculated by linearly fitting the log of the FFT-estimated gain, $\ln(G)$, to the distance along the undulator, as shown in Fig. 5. The inverse of this slope is the gain length, simulated here with system jitter of Table 2 and nominal 1.2-μm emittance, producing a fitted gain length of $L_G \approx 4.46 \pm 0.08$ m, whereas the average gain length in simulation is 4.33 m, a reasonable agreement within 1.6 standard deviations.

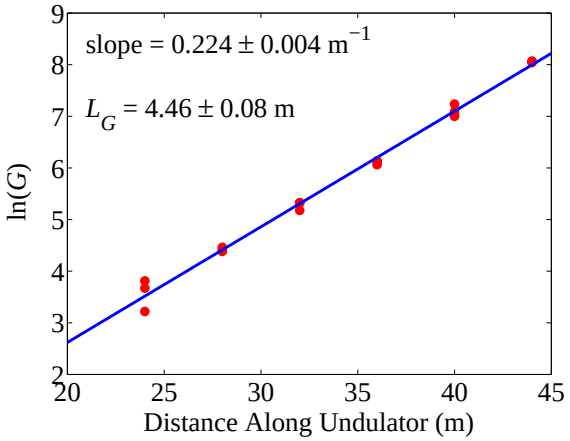

Figure 5: Log of estimated gain, G, plotted along undulator at a very early stage of the FEL, including machine jitter. The gain length estimate from this is $L_G = 4.46 \pm 0.08$ m.

In this case the gain is measured starting at a point along the undulator (24 m) where the gain is only $G \approx 25$. In this way the gain length might be measured at early locations along the undulator where the gain is low, and the linearity of the logarithmic curve might be used to search for weak sections of the undulator which may indicate local undulator or trajectory errors.

ACKNOWLEDGMENTS

We thank useful discussions with K. Robinson, J. Rossbach, and G. Stupakov. This work was supported by Department of Energy contract DE–AC02–76SF00515.

REFERENCES

[1] Linac Coherent Light Source Conceptual Design Report, SLAC-R-593, UC-414 (2002).

[2] Z. Huang *et al.* Phys. Rev. ST Accel. Beams **7**, 074401 (2004).

[3] K. Robinson, private communication.

[4] G. Stupakov, private communication.

[5] M. Xie, Proceedings of the 1995 Particle Accelerator Conference, 183 (1995).

[6] K.-J. Kim, Phys. Rev. Lett. **57**, 1871 (1986).

[7] P. Emma et al., SLAC-PUB-8864, June 2001.